

- Journal of Building Engineering*, 47(October 2021), 103880. <https://doi.org/10.1016/j.jobe.2021.103880>
- Salkhordeh, M., Govahi, E., & Mirtaheri, M. (2021). Seismic fragility evaluation of various mitigation strategies proposed for bridge piers. *Structures*, 33(May), 1892–1905. <https://doi.org/10.1016/j.istruc.2021.05.041>
- Shama, A., & Jones, M. (2020). Seismic Performance-Based Design of Cable-Supported Bridges: State of Practice in the United States. *Journal of Bridge Engineering*, 25(12), 1–10. [https://doi.org/10.1061/\(asce\)be.1943-5592.0001639](https://doi.org/10.1061/(asce)be.1943-5592.0001639)
- Shirwa, A. M., Moniruzzaman, P., Biswas, T., & Shirwa, A. (2014). *Incremental Dynamic Analysis of Reinforced Concrete Structures Considering Height Effects*. October 2014, 0–9.
- Simanjuntak, A. V. H., Asnawi, Y., Umar, M., Rizal, S., & Syukri, M. (2020). A Microtremor Survey to Identify Seismic Vulnerability Around Banda Aceh Using HVSR Analysis. *Elkawnie*, 6(2), 342. <https://doi.org/10.22373/ekw.v6i2.7886>
- Simos, N., Manos, G. C., & Kozikopoulos, E. (2018). Near- and far-field earthquake damage study of the Konitsa stone arch bridge. *Engineering Structures*, 177, 256–267. <https://doi.org/10.1016/j.engstruct.2018.09.072>
- Society, S. (1976). A study on the duration of strong earthquake ground motion. 14F, 1T, Refs. *International Journal of Rock Mechanics and Mining Sciences & Geomechanics Abstracts*, 13(3), 28. [https://doi.org/10.1016/0148-9062\(76\)90487-3](https://doi.org/10.1016/0148-9062(76)90487-3)
- Soltangharaei, V., Razi, M., & Gerami, M. (2016). Comparative evaluation of behavior factor of SMRF structures for near and far fault ground motions. *Periodica Polytechnica Civil Engineering*, 60(1), 75–82. <https://doi.org/10.3311/PPci.7625>
- Somerville, P. (1999). *Characterizing Crustal Earthquake Slip Models for the Prediction of Strong Ground Motion*. October 2016. <https://doi.org/10.1785/gssrl.70.1.59>
- Soyluk, K., & Karaca, H. (2017). Near-fault and far-fault ground motion effects on cable-supported bridges. *Procedia Engineering*, 199, 3077–3082. <https://doi.org/10.1016/j.proeng.2017.09.421>
- Su, P., Zhu, X., Chen, Y., Xue, B., & Zhang, B. (2022). Seismic Response Analysis of a Curved Bridge under Near-Fault and Far-Field Ground Motions. *Applied Sciences*, 12(16), 8349. <https://doi.org/10.3390/app12168349>
- Sucuoğlu, H., & Nurtuğ, A. (1995). Earthquake ground motion characteristics and seismic energy dissipation. *Earthquake Engineering & Structural Dynamics*, 24(9), 1195–1213. <https://doi.org/10.1002/eqe.4290240903>
- Sucuoğlu, H., Yüçemen, S., Gezer, A., & Erberik, A. (1998). Statistical evaluation of the damage potential of earthquake ground motions. *Structural Safety*, 20(4), 357–378. [https://doi.org/10.1016/S0167-4730\(98\)00018-6](https://doi.org/10.1016/S0167-4730(98)00018-6)
- Sun, B., Zhang, S., Deng, M., & Wang, C. (2020). Inelastic dynamic response and fragility analysis of arched hydraulic tunnels under as-recorded far-fault and near-fault ground motions. *Soil Dynamics and Earthquake*

- Engineering*, 132(December 2019), 106070.  
<https://doi.org/10.1016/j.soildyn.2020.106070>
- Tauheed, A., & Alam, M. (2022). Seismic performance of regular frame under near field and far field earthquakes. *Materials Today: Proceedings*, 64, 554–569. <https://doi.org/10.1016/j.matpr.2022.05.112>
- Tehrani, P., & Mitchell, D. (2013). Incremental dynamic analysis (IDA) applied to seismic risk assessment of bridges. *Handbook of Seismic Risk Analysis and Management of Civil Infrastructure Systems*, March 2016, 561–596. <https://doi.org/10.1533/9780857098986.4.561>
- Thachampuram, S. J. (2014). *Development of Fragility Curves for an RC Frame*. 6890(May), 591–594.
- Todorov, B., & Billah, A. H. M. M. (2021). Seismic fragility and damage assessment of reinforced concrete bridge pier under long-duration, near-fault, and far-field ground motions. *Structures*, 31, 671–685. <https://doi.org/10.1016/j.istruc.2021.02.019>
- Towashiraporn, P., & Disaster, A. (2012). *Earthquake Risk Assessment of Mandalay City, Myanmar*.
- Tubaldi, E., Dall'Asta, A., & Dezi, L. (2015). Seismic response analysis of continuous multispan bridges with partial isolation. *Shock and Vibration*, 2015. <https://doi.org/10.1155/2015/183756>
- Tubaldi, E., Scozzese, F., De Domenico, D., & Dall'Asta, A. (2021). Effects of axial loads and higher order modes on the seismic response of tall bridge piers. *Engineering Structures*, 247(April), 113134. <https://doi.org/10.1016/j.engstruct.2021.113134>
- Vamvatsikos, D. (2018). *Applied Incremental Dynamic Analysis* 1. April. <https://doi.org/10.1193/1.1737737>
- Vamvatsikos, D., & Cornell, C. A. (2004). Applied incremental dynamic analysis. *Earthquake Spectra*, 20(2), 523–553. <https://doi.org/10.1193/1.1737737>
- Van Der Elst, N. J., & Brodsky, E. E. (2010). Connecting near-field and far-field earthquake triggering to dynamic strain. *Journal of Geophysical Research: Solid Earth*, 115(7), 1–21. <https://doi.org/10.1029/2009JB006681>
- Vargas, Y. F., Barbat, A. H., Pujades, L. G., & Hurtado, J. E. (2014). Probabilistic seismic risk evaluation of reinforced concrete buildings. *Proceedings of the Institution of Civil Engineers: Structures and Buildings*, 167(6), 327–336. <https://doi.org/10.1680/stbu.12.00031>
- Vargas, Y. F., Pujades, L. B., Barbat, A. H., & Hurtado, J. E. (2010). Probabilistic assessment of the global damage in reinforced concrete structures. *14Ecee*, 43–61.
- Vargas, Y. F., Pujades, L. G., Barbat, A. H., & Hurtado, J. E. (2013). Capacity, fragility and damage in reinforced concrete buildings: A probabilistic approach. *Bulletin of Earthquake Engineering*, 11(6), 2007–2032. <https://doi.org/10.1007/s10518-013-9468-x>
- Vazurkar, U. Y., & Chaudhari, D. J. (2016). Development of Fragility Curves for RC Buildings. *International Journal of Engineering Research*, 5(Special 3), 591–594.

- Veggalam, S., Karthik Reddy, K. S. K., & Somalia, S. N. (2021). Collapse fragility due to near-field directivity ground motions: Influence of component, rupture distance, hypocenter location. *Structures*, 34(September), 3684–3702. <https://doi.org/10.1016/j.istruc.2021.09.096>
- Verma, I., & Kumar, A. (2021). *Analytical Study on Ductility Parameters of seismic resisting elements*. November 2021, 16571–16582.
- Vona, M. (2014). Fragility Curves of Existing RC Buildings Based on Specific Structural Performance Levels. *Open Journal of Civil Engineering*, 04(02), 120–134. <https://doi.org/10.4236/ojce.2014.42011>
- Wei, B., Zuo, C., He, X., Jiang, L., & Wang, T. (2018). Effects of vertical ground motions on seismic vulnerabilities of a continuous track-bridge system of high-speed railway. *Soil Dynamics and Earthquake Engineering*, 115(September), 281–290. <https://doi.org/10.1016/j.soildyn.2018.08.022>
- Wu, S. L., Charatpangoon, B., Kiyono, J., Maeda, Y., Nakatani, T., & Li, S. Y. (2016). Synthesis of near-fault ground motion using a hybrid method of stochastic and theoretical green's functions. *Frontiers in Built Environment*, 2(October). <https://doi.org/10.3389/fbuil.2016.00024>
- Xu, J. G., Cai, Z. K., & Feng, D. C. (2021). Life-cycle seismic performance assessment of aging RC bridges considering multi-failure modes of bridge columns. *Engineering Structures*, 244(January), 112818. <https://doi.org/10.1016/j.engstruct.2021.112818>
- Yang, S., & Mavroeidis, G. P. (2018a). Bridges crossing fault rupture zones: A review. *Soil Dynamics and Earthquake Engineering*, 113(February), 545–571. <https://doi.org/10.1016/j.soildyn.2018.03.027>
- Yang, S., & Mavroeidis, G. P. (2018b). Bridges crossing fault rupture zones: A review. *Soil Dynamics and Earthquake Engineering*, 113(July), 545–571. <https://doi.org/10.1016/j.soildyn.2018.03.027>
- Yilmaza, M. F., & Alpaslanb, E. (2020). Civil Engineering Beyond Limits. *Acapublishing.Com*, 1, 22–28.
- Zhang, Q., & Alam, M. S. (2020). State-of-the-Art Review of Seismic-Resistant Precast Bridge Columns. *Journal of Bridge Engineering*, 25(10), 1–16. [https://doi.org/10.1061/\(asce\)be.1943-5592.0001620](https://doi.org/10.1061/(asce)be.1943-5592.0001620)
- Zheng, S. xiong, Shi, X. hu, Jia, H. yu, Zhao, C. hui, Qu, H. lue, & Shi, X. long. (2020). Seismic response analysis of long-span and asymmetrical suspension bridges subjected to near-fault ground motion. *Engineering Failure Analysis*, 115(May). <https://doi.org/10.1016/j.engfailanal.2020.104615>
- Zheng, S. xiong, Shi, X. long hu, Jia, H. yu, Zhao, C. hui, Qu, H. lue, Shi, X. long hu, Todorov, B., Billah, A. H. M. M., Noori, H. R., Memarpour, M. M., Yakhchalian, M., Soltanieh, S., Chen, X., Xiang, N., Li, C., Nazarnezhad, T., Naderpour, H., Chen, X., Li, C., ... Somalia, S. N. (2021). Deriving seismic fragility curves for sheet-pile wharves using finite element analysis. *Structures*, 115(January), 265–277. <https://doi.org/10.1016/j.soildyn.2019.105945>

Zou, P. X. W. (2003). Flexural Behavior and Deformability of Fiber Reinforced Polymer Prestressed Concrete Beams. *Journal of Composites for Construction*, 7(4), 275–284. [https://doi.org/10.1061/\(asce\)1090-0268\(2003\)7:4\(275\)](https://doi.org/10.1061/(asce)1090-0268(2003)7:4(275))





## APPENDIX-A

### Appendix-A.1.Material Properties and Section Properties

Concrete Material	
con_ma	Mander et al. nonlinear concrete model
Compressive Strength	45 MPa
Modulus of Elasticity of Concrete	26300 MPa
Steel Material	
stl_mp	Menegotto-Pinto steel model
Yield Strength	500 MPa
Modulus of Elasticity of Steel	200,000 MPa
Unit Weight of Reinforced Concrete	2.5 ton/m <sup>3</sup>
Unit Weight of Wearing Surface	2.25 ton/m <sup>3</sup>
Section Properties	
Pier	Reinforced Concrete Rectangular Hollow Section
Slab thickness	0.25m
Parapet Height	1.445 m
Diaphragm Height	1.25 m
Diaphragm Width	0.40 m
Girder	PCI Girders
Pier Head Height	4 m
Pier Head Width	3.9 m
Element Classes	
Inelastic Force-based Frame Element (infrmFB)	Piers
Elastic Frame Element (elfrm)	Rigid Link for Piers and Pier Heads Decking Pier Head Diaphragm
Linear-Symmetric	Pier Head to Slab

### Appendix-A.2.Mass of Piers

**The Whole Mass of Piers**

Sr. No.	Item	Length L (m)	Breadth B (m)	Thickness H (m)	Density of RC γ (ton/m <sup>3</sup> )	Mass (LxBxHγ) (ton)
1	Pier 1	29.338	3.10	3.600	2.50	818.53
2	Pier 2	42.810	3.10	3.600	2.50	1194.40
3	Pier 3	42.810	3.10	3.600	2.50	1194.40
4	Pier 4	46.451	3.10	3.600	2.50	1295.98

**The Middle Mass of Piers**

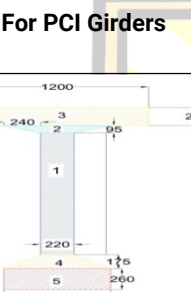
Sr. No.	Item	Length L (m)	Breadth B (m)	Thickness H (m)	Density (ton/m <sup>3</sup> )	Mass (LxBxHγ) (ton)
1	Pier 1	29.338	3.10	2.600	2.50	591.16
2	Pier 2	42.810	3.10	2.600	2.50	862.62
3	Pier 3	42.810	3.10	2.600	2.50	862.62
4	Pier 4	46.451	3.10	2.600	2.50	935.99

### Appendix-A.2 Continued:

#### Lumped Mass of Piers

Sr. No.	Item	Whole Mass (ton)	Middle Mass (ton)	Lumped Mass (ton)
1	Pier 1	818.53	591.16	227.37
2	Pier 2	1194.40	862.62	331.78
3	Pier 3	1194.40	862.62	331.78
4	Pier 4	1295.98	935.99	360.00

### Appendix-A.3.PCI Girder Area

For PCI Girders	Area 1 ( $m^2$ )	Area 2 ( $m^2$ )	Area 3 ( $m^2$ )	Area 4 ( $m^2$ )	Area 5 ( $m^2$ )	Total Area ( $m^2$ )
	0.33	0.04	0.27	0.08	0.18	0.91

### Appendix-A.4.Load calculation

Sr. No .	Item	Total Number	Length L (m)	Breadth B (m)	Thickness s H (m)	Density γ (ton/m <sup>3</sup> )	Distributed load (ton/m)
							B x H x γ
1	Girder	1	196.2	0.91 (m <sup>2</sup> )		2.50	2.275
2	Pier Head	1	28.200	2.15	3.100	2.50	16.66
3	Diaphragm	1	11.200	0.40	3.030	2.50	3.03
4	Slab	1	196.2	11.245	0.25	2.5	7.028
5	Parapet	1	196.2	0.502 (m <sup>2</sup> )		2.5	1.278
6	Asphalt Wearing Surface	1	196.2	11.245	0.08	2.25	2.024

## APPENDIX-B

### Appendix-B.1.Nodes

Node Name	X	Y	Z	Type
A1*	0	6.95	-0.01	non-structural
A1**	0	21.25	-0.01	non-structural
L4a	154.2	21.25	0	structural
l1a	38.1	21.25	0	structural
ns	-0.01	6.95	0	non-structural
ns*	-0.01	21.25	0	non-structural
p1	38.1	6.95	0	structural
l1	38.1	6.95	0	structural
A1	0	6.95	3.513	structural
l2	76.8	6.95	0	structural
A2	196.2	6.95	3.513	structural
l3	115.5	6.95	0	structural
d3	38.1	6.95	3.513	structural
l4	154.2	6.95	0	structural
d6	76.8	6.95	3.513	structural
d9	115.5	6.95	3.513	structural
A11	0	21.25	3.513	structural
d12	154.2	6.95	3.513	structural
A22	196.2	21.25	3.513	structural
d23	38.1	21.25	3.513	structural
d26	76.8	21.25	3.513	structural
d29	115.5	21.25	3.513	structural
d32	154.2	21.25	3.513	structural
l2a	76.8	21.25	0	structural
l3a	115.5	21.25	0	structural
p1*	38.1	6.95	-29.338	non-structural
p1**	38.1	6.95	-30.938	structural
p1a	38.1	21.25	0	structural
p1a*	38.1	21.25	-29.338	non-structural
p1a**	38.1	21.25	-30.938	structural
p2	76.8	6.95	0	structural
p2*	76.8	6.95	-42.8	non-structural
p2**	76.8	6.95	-44.41	structural
p2a	76.8	21.25	0	structural
p2a*	76.8	21.25	-42.8	non-structural
p2a**	76.8	21.25	-44.41	structural
p3	115.5	6.95	0	structural
p3*	115.5	6.95	-42.81	non-structural
p3**	115.5	6.95	-44.41	structural
p3a	115.5	21.25	0	structural
p3a*	115.5	21.25	-42.81	non-structural
p3a**	115.5	21.25	-44.41	structural
p4	154.2	6.95	0	structural
p4*	154.2	6.95	-46.451	non-structural
p4**	154.2	6.95	-48.051	structural
p4a	154.2	21.25	0	structural
p4a*	154.2	21.25	-46.451	non-structural
p4a**	154.2	21.25	-48.051	structural

**Appendix-B.1 Continued:**

Node Name	X	Y	Z	Type
ph1	38.1	0	0	structural
ph1*	38.1	28.2	0	structural
ph2	76.8	0	0	structural
ph2*	76.8	28.2	0	structural
ph3	115.5	0	0	structural
ph3*	115.5	28.2	0	structural
ph4	154.2	0	0	structural
ph4*	154.2	28.2	0	structural

**Appendix-B.2.Element Connectivity**

Element Name	Element Class	Node Names	Rigid Offset
Link1*	phpierlink	l1a p1a A11 ns*	-
Link2*	phpierlink	l2a p2a A11 ns*	-
Link3*	phpierlink	l3a p3a A11 ns	-
Link4*	phpierlink	l4a p4a A11 ns	-
Pdm1	Ldeckmass	p1	-
Pdm1a	Ldeckmass	p1a	-
Pdm2a	Ldeckmass	p2a	-
Pdm3a	Ldeckmass	p3a	-
Pdm4a	Ldeckmass	p4a	-
Pier1	Pier11	p1 p1** deg=180.00	0.00 0.00 0.00 0.00 0.00 0.00 0.00
Pm1	Lmaspr1	p1	-
PierHead1	PierHead	ph1 p1 deg=0.00	0.00 0.00 0.00 0.00 0.00 0.00 0.00
Link1	phpierlink	l1 p1 A1 ns	-
PierHead2	PierHead	p1 p1a deg=0.00	0.00 0.00 0.00 0.00 0.00 0.00 0.00
Pdm2	Ldeckmass	p2	-
Link2	phpierlink	l2 p2 A1 ns	-
Pier2	Pier22	p2 p2** deg=180.00	0.00 0.00 0.00 0.00 0.00 0.00 0.00
Pm1a	Lmaspr1	p1a	-
Pm2	Lmaspr2	p2	-
Pdm3	Ldeckmass	p3	-
Link3	phpierlink	l3 p3 A1 ns	-
PierHead3	PierHead	p1a ph1* deg=0.00	0.00 0.00 0.00 0.00 0.00 0.00 0.00
Pier3	Pier33	p3 p3** deg=180.00	0.00 0.00 0.00 0.00 0.00 0.00 0.00
Pm3	Lmaspr3	p3	-
Pdm4	Ldeckmass	p4	-
Link4	phpierlink	l4 p4 A1 ns	-
PierHead4	PierHead	ph2 p2 deg=0.00	0.00 0.00 0.00 0.00 0.00 0.00 0.00
Pier4	Pier44	p4 p4** deg=180.00	0.00 0.00 0.00 0.00 0.00 0.00 0.00
PierHead5	PierHead	p2 p2a deg=0.00	0.00 0.00 0.00 0.00 0.00 0.00 0.00
PierHead6	PierHead	p2a ph2* deg=0.00	0.00 0.00 0.00 0.00 0.00 0.00 0.00
PierHead7	PierHead	ph3 p3 deg=0.00	0.00 0.00 0.00 0.00 0.00 0.00 0.00
PierHead8	PierHead	p3 p3a deg=0.00	0.00 0.00 0.00 0.00 0.00 0.00 0.00
PierHead9	PierHead	p3a ph3* deg=0.00	0.00 0.00 0.00 0.00 0.00 0.00 0.00
PierHead10	PierHead	ph4 p4 deg=0.00	0.00 0.00 0.00 0.00 0.00 0.00 0.00

### Appendix-B.2 Continued

Element Name	Element Class	Node Names	Rigid Offset						
PierHead11	PierHead	p4 p4a deg=0.00	0.00 0.00 0.00 0.00 0.00 0.00 0.00						
Pier11	Pier11	p1a p1a** deg=180.00	0.00 0.00 0.00 0.00 0.00 0.00 0.00						
PierHead12	PierHead	p4a ph4* deg=0.00	0.00 0.00 0.00 0.00 0.00 0.00 0.00						
Pier22	Pier22	p2a p2a** deg=180.00	0.00 0.00 0.00 0.00 0.00 0.00 0.00						
Pier33	Pier33	p3a p3a** deg=180.00	0.00 0.00 0.00 0.00 0.00 0.00 0.00						
Pier44	Pier44	p4a p4a** deg=180.00	0.00 0.00 0.00 0.00 0.00 0.00 0.00						
Pm2a	Lmaspr2	p2a	-						
Pm3a	Lmaspr3	p3a	-						
Pm4a	Lmaspr4	p4a	-						
dm1	distribdeck	A1 d3	-						
Rigid1	RigidPiPh	p1 d3 deg=180.00	0.00 0.00 0.00 0.00 0.00 0.00 0.00						
deck1	decking	A1 d3 deg=0.00	0.00 0.00 0.00 0.00 0.00 0.00 0.00						
dm2	distribdeck	d3 d6	-						
deck2	decking	d3 d6 deg=0.00	0.00 0.00 0.00 0.00 0.00 0.00 0.00						
Rigid2	RigidPiPh	p1a d23 deg=180.00	0.00 0.00 0.00 0.00 0.00 0.00 0.00						
Rigid3	RigidPiPh	p2 d6 deg=180.00	0.00 0.00 0.00 0.00 0.00 0.00 0.00						
deck3	decking	d6 d12 deg=0.00	0.00 0.00 0.00 0.00 0.00 0.00 0.00						
dm3	distribdeck	d6 d12	-						
Pm4	Lmaspr4	p4	-						
dm4	distribdeck	d12 A2	-						
deck4	decking	d12 A2 deg=0.00	0.00 0.00 0.00 0.00 0.00 0.00 0.00						
Rigid4	RigidPiPh	p2a d26 deg=180.00	0.00 0.00 0.00 0.00 0.00 0.00 0.00						
deck5	decking	A11 d23 deg=0.00	0.00 0.00 0.00 0.00 0.00 0.00 0.00						
dm5	distribdeck	A11 d23	-						
Rigid5	RigidPiPh	p3 d9 deg=180.00	0.00 0.00 0.00 0.00 0.00 0.00 0.00						
dm6	distribdeck	d23 d26	-						
deck6	decking	d23 d26 deg=0.00	0.00 0.00 0.00 0.00 0.00 0.00 0.00						
Rigid6	RigidPiPh	p3a d29 deg=180.00	0.00 0.00 0.00 0.00 0.00 0.00 0.00						
deck7	decking	d26 d29 deg=0.00	0.00 0.00 0.00 0.00 0.00 0.00 0.00						
Rigid7	RigidPiPh	p4 d12 deg=180.00	0.00 0.00 0.00 0.00 0.00 0.00 0.00						
dm7	distribdeck	d26 d29	-						
dm8	distribdeck	d29 d32	-						
Rigid8	RigidPiPh	p4a d32 deg=180.00	0.00 0.00 0.00 0.00 0.00 0.00 0.00						
deck8	decking	d29 d32 deg=0.00	0.00 0.00 0.00 0.00 0.00 0.00 0.00						
deck9	decking	d32 A22 deg=0.00	0.00 0.00 0.00 0.00 0.00 0.00 0.00						
dm9	distribdeck	d32 A22	-						

### Appendix-B.3.Restraints

<b>Nodes Name</b>	<b>Restraints</b>	<b>Nodes Name</b>	<b>Restraints</b>
A1	$y+z+rx+rz$	p3**	$x+y+z+rx+ry+rz$
A1*	non-structural	p3a	
A1**	non-structural	p3a*	non-structural
A2	$x+y+z+rx+rz$	p3a**	$x+y+z+rx+ry+rz$
L4a		p4	
ns	non-structural	p4*	non-structural
ns*	non-structural	p4**	$x+y+z+rx+ry+rz$
I1		p4a	
p1		p4a*	non-structural
I2		p4a**	$x+y+z+rx+ry+rz$
I3		ph1	
d3		ph1*	
I4		ph2	
d6		ph2*	
d9		ph3	
A11	$y+z+rx+rz$	ph3*	
d12		ph4	
A22	$x+y+z+rx+rz$	ph4*	
d23			
d26			
d29			
d32			
I1a			
I2a			
I3a			
p1*	non-structural		
p1**	$x+y+z+rx+ry+rz$		
p1a			
p1a*	non-structural		
p1a**	$x+y+z+rx+ry+rz$		
p2			
p2*	non-structural		
p2**	$x+y+z+rx+ry+rz$		
p2a*	non-structural		
p2a**	$x+y+z+rx+ry+rz$		
p2a			
p3			
p3*	non-structural		

## APPENDIX-C

### Appendix-C.1.Modal Periods and Frequencies

Mode	Period (sec)	Frequency (Hertz)	Angular Frequency (rad/sec)
1	0.83449556	1.19832872	7.5293214
2	0.53902914	1.85518727	11.65648541
3	0.43787658	2.28374855	14.34921537
4	0.34862248	2.86843231	18.02289177
5	0.27299798	3.66303082	23.01550143
6	0.21716081	4.60488238	28.93332932
7	0.16739271	5.97397566	37.5355961
8	0.15182811	6.58639551	41.38354353
9	0.13441811	7.43947362	46.74359137
10	0.12623736	7.92158512	49.77278723
11	0.12351903	8.09591837	50.86815537
12	0.1155957	8.65084072	54.3548353
13	0.11527596	8.67483552	54.50559908
14	0.10805343	9.25468113	58.1488765
15	0.10781149	9.27544883	58.27936378
16	0.09464275	10.56604942	66.38844646
17	0.08861991	11.28414598	70.90038024
18	0.08818754	11.33947077	71.24799614
19	0.08467393	11.81001115	74.20448853
20	0.07443246	13.43499917	84.41458938
21	0.07324158	13.65344574	85.78712967
22	0.07260029	13.77405038	86.54491097
23	0.0705915	14.16601063	89.00766984
24	0.0662414	15.09629848	94.85284078
25	0.06444248	15.51771551	97.5006821
26	0.06257004	15.98208969	100.4184311
27	0.06071673	16.46992632	103.4835991
28	0.05226432	19.13351339	120.2194102
29	0.0479178	20.8690717	131.1242447
30	0.03921528	25.50026479	160.222889
31	0.03749883	26.66749725	167.5568269
32	0.03658287	27.33519528	171.7520973
33	0.03005563	33.27163135	209.0518252
34	0.02416938	41.37465849	259.9646463
35	0.02333796	42.8486421	269.2259585
36	0.0196157	50.97957174	320.3140961

**Appendix-C.2.Longitudinal Axis Displacement Capacity Curves due to Targt Displacement in Longitudinal Direction Data Ouput**

Sr No.	Displacement (m)	Base Shear (kN)	Sr No.	Displacement (m)	Base Shear (kN)	Sr No.	Displacement (m)	Base Shear (kN)
1	0	0	43	0.21	252356	85	0.42	218665
2	0.005	14363	44	0.215	254201	86	0.425	218159
3	0.01	27844	45	0.22	255793	87	0.43	217646
4	0.015	39330	46	0.225	257166	88	0.435	217136
5	0.02	49432	47	0.23	258358	89	0.44	216636
6	0.025	58536	48	0.235	259366	90	0.445	216147
7	0.03	67023	49	0.24	260181	91	0.45	215669
8	0.035	74994	50	0.245	260766	92	0.455	215202
9	0.04	82538	51	0.25	261108	93	0.46	214746
10	0.045	89797	52	0.255	261122	94	0.465	214297
11	0.05	96755	53	0.26	260560	95	0.47	213858
12	0.055	103523	54	0.265	259258	96	0.475	213427
13	0.06	110118	55	0.27	258066	97	0.48	212997
14	0.065	116611	56	0.275	256812	98	0.485	212554
15	0.07	123048	57	0.28	255764	99	0.49	212050
16	0.075	129413	58	0.285	254756	100	0.495	211394
17	0.08	135720	59	0.29	253796	101	0.5	210197
18	0.085	141983	60	0.295	252838			
19	0.09	148181	61	0.3	251839			
20	0.095	154296	62	0.305	250742			
21	0.1	160313	63	0.31	249523			
22	0.105	166211	64	0.315	248125			
23	0.11	171989	65	0.32	246422			
24	0.115	177650	66	0.325	244547			
25	0.12	183172	67	0.33	242115			
26	0.125	188560	68	0.335	238355			
27	0.13	193801	69	0.34	234960			
28	0.135	198873	70	0.345	232275			
29	0.14	203760	71	0.35	229728			
30	0.145	208473	72	0.355	228123			
31	0.15	213011	73	0.36	226800			
32	0.155	217379	74	0.365	225741			
33	0.16	221554	75	0.37	224789			
34	0.165	225544	76	0.375	223911			
35	0.17	229346	77	0.38	223105			
36	0.175	232931	78	0.385	222463			
37	0.18	236322	79	0.39	221880			
38	0.185	239525	80	0.395	221314			
39	0.19	242531	81	0.4	220767			
40	0.195	245320	82	0.405	220230			
41	0.2	247886	83	0.41	219701			
42	0.205	250233	84	0.415	219180			

**Appendix-C.3.Transverse Axis Displacement Capacity Curves due to Targt Displacement in Longitudinal Direction Data Ouput**

Sr No.	Displacement (m)	Base Shear (kN)	Sr No.	Displacement (m)	Base Shear (kN)	Sr No.	Displacement (m)	Base Shear (kN)
1	0	0	43	0.21	145338	85	0.42	218548
2	0.005	5360	44	0.215	147947	86	0.425	220502
3	0.01	10457	45	0.22	150477	87	0.43	222499
4	0.015	14914	46	0.225	152929	88	0.435	224523
5	0.02	18881	47	0.23	155289	89	0.44	226543
6	0.025	22620	48	0.235	157552	90	0.445	228556
7	0.03	26235	49	0.24	159712	91	0.45	230560
8	0.035	29808	50	0.245	161740	92	0.455	232553
9	0.04	33329	51	0.25	163578	93	0.46	234534
10	0.045	36842	52	0.255	165182	94	0.465	236494
11	0.05	40354	53	0.26	166341	95	0.47	238422
12	0.055	43858	54	0.265	167086	96	0.475	240312
13	0.06	47378	55	0.27	168247	97	0.48	242150
14	0.065	50905	56	0.275	169505	98	0.485	243901
15	0.07	54430	57	0.28	171032	99	0.49	245523
16	0.075	57955	58	0.285	172658	100	0.495	246972
17	0.08	61487	59	0.29	174388	101	0.5	248069
18	0.085	65017	60	0.295	176167			
19	0.09	68543	61	0.3	177995			
20	0.095	72064	62	0.305	179849			
21	0.1	75575	63	0.31	181731			
22	0.105	79076	64	0.315	183584			
23	0.11	82563	65	0.32	185296			
24	0.115	86032	66	0.325	186988			
25	0.12	89486	67	0.33	188358			
26	0.125	92915	68	0.335	189040			
27	0.13	96315	69	0.34	189729			
28	0.135	99684	70	0.345	190636			
29	0.14	103023	71	0.35	191755			
30	0.145	106330	72	0.355	193567			
31	0.15	109600	73	0.36	195435			
32	0.155	112827	74	0.365	197317			
33	0.16	116014	75	0.37	199213			
34	0.165	119163	76	0.375	201122			
35	0.17	122276	77	0.38	203045			
36	0.175	125335	78	0.385	204958			
37	0.18	128349	79	0.39	206876			
38	0.185	131317	80	0.395	208805			
39	0.19	134230	81	0.4	210743			
40	0.195	137095	82	0.405	212688			
41	0.2	139905	83	0.41	214638			
42	0.205	142655	84	0.415	216591			

**Appendix-C.4.Longitudinal Axis Displacement Capacity Curves due to Targt Displacement in Transverse Direction Data Output**

Sr. No.	Displacement (m)	Base Shear (kN)	Sr. No.	Displacement (m)	Base Shear (kN)	Sr. No.	Displacement (m)	Base Shear (kN)
1	0.000	0	40	0.137	200388	79	0.273	257337
2	0.004	10048	41	0.140	203785	80	0.277	256507
3	0.007	20027	42	0.144	207097	81	0.280	255801
4	0.011	29074	43	0.147	210324	82	0.284	255088
5	0.014	37162	44	0.151	213468	83	0.287	254413
6	0.018	44573	45	0.154	216525	84	0.291	253751
7	0.021	51351	46	0.158	219493	85	0.294	253088
8	0.025	57700	47	0.161	222368	86	0.298	252407
9	0.028	63733	48	0.165	225153	87	0.301	251695
10	0.032	69518	49	0.168	227846	88	0.305	250929
11	0.035	75055	50	0.172	230435	89	0.308	250105
12	0.039	80368	51	0.175	232924	90	0.312	249202
13	0.042	85563	52	0.179	235317	91	0.315	248202
14	0.046	90583	53	0.182	237617	92	0.319	247058
15	0.049	95463	54	0.186	239825	93	0.322	245789
16	0.053	100256	55	0.189	241937	94	0.326	244415
17	0.056	104953	56	0.193	243942	95	0.329	242755
18	0.060	109568	57	0.196	245841	96	0.333	240332
19	0.063	114129	58	0.200	247627	97	0.336	237732
20	0.067	118668	59	0.203	249304	98	0.340	235281
21	0.070	123171	60	0.207	250877	99	0.343	233458
22	0.074	127639	61	0.210	252339	100	0.347	231493
23	0.077	132078	62	0.214	253661			
24	0.081	136488	63	0.217	254845			
25	0.084	140876	64	0.221	255920			
26	0.088	145231	65	0.224	256886			
27	0.091	149550	66	0.228	257768			
28	0.095	153821	67	0.231	258556			
29	0.098	158047	68	0.235	259256			
30	0.102	162216	69	0.238	259866			
31	0.105	166327	70	0.242	260366			
32	0.109	170375	71	0.245	260754			
33	0.112	174366	72	0.249	261024			
34	0.116	178296	73	0.252	261158			
35	0.119	182153	74	0.256	261094			
36	0.123	185946	75	0.259	260749			
37	0.126	189675	76	0.263	259925			
38	0.130	193329	77	0.266	259065			
39	0.133	196901	78	0.270	258233			

**Appendix-C.5.Transverse Axis Displacement Capacity Curves due to Targt Displacement in Transverse Direction Data Ouput**

Sr. No.	Displacement (m)	Base Shear (kN)	Sr. No.	Displacement (m)	Base Shear (kN)	Sr. No.	Displacement (m)	Base Shear (kN)
1	0.000	0	42	0.144	105333	82	0.284	172089
2	0.004	3733	43	0.147	107636	83	0.287	173270
3	0.007	7486	44	0.151	109916	84	0.291	174496
4	0.011	10929	45	0.154	112177	85	0.294	175742
5	0.014	14072	46	0.158	114417	86	0.298	177009
6	0.018	16937	47	0.161	116639	87	0.301	178297
7	0.021	19645	48	0.165	118842	88	0.305	179597
8	0.025	22254	49	0.168	121027	89	0.308	180912
9	0.028	24798	50	0.172	123190	90	0.312	182229
10	0.032	27310	51	0.175	125328	91	0.315	183520
11	0.035	29809	52	0.179	127441	92	0.319	184746
12	0.039	32277	53	0.182	129533	93	0.322	185935
13	0.042	34731	54	0.186	131602	94	0.326	187083
14	0.046	37194	55	0.189	133641	95	0.329	188065
15	0.049	39652	56	0.193	135660	96	0.333	188674
16	0.053	42107	57	0.196	137652	97	0.336	189123
17	0.056	44560	58	0.200	139617	98	0.340	189571
18	0.060	47025	59	0.203	141554	99	0.343	190234
19	0.063	49494	60	0.207	143456	100	0.347	190826
20	0.067	51962	61	0.210	145329	101	0.350	191698
21	0.070	54429	62	0.214	147163			
22	0.074	56895	63	0.217	148958			
23	0.077	59366	64	0.221	150717			
24	0.081	61839	65	0.224	152436			
25	0.084	64309	66	0.228	154107			
26	0.088	66777	67	0.231	155736			
27	0.091	69242	68	0.235	157315			
28	0.095	71706	69	0.238	158844			
29	0.098	74165	70	0.242	160317			
30	0.102	76619	71	0.245	161720			
31	0.105	79068	72	0.249	163026			
32	0.109	81511	73	0.252	164248			
33	0.112	83945	74	0.256	165299			
34	0.116	86370	75	0.259	166143			
35	0.119	88790	76	0.263	166619			
36	0.123	91197	77	0.266	167287			
37	0.126	93590	78	0.270	168098			
38	0.130	95968	79	0.273	168934			
39	0.133	98332	80	0.277	169877			
40	0.137	100681	81	0.280	170969			

**Appendix-C.6.Four Damage States Probability of Exceeding on Spectral Displacement Longitudinal Direction due to Target Displacement in Transverse Direction by POA**

Slight (Sd <sub>1</sub> )	$\beta$	Ln(Sd <sub>1</sub> )	Ln( $\lambda$ )	Ln(Sd <sub>1</sub> )-Ln( $\lambda$ )	(Ln(Sd <sub>1</sub> )-Ln( $\lambda$ ))/ $\beta$	Probability
0.060700	0.0173	-2.8018	-2.6493	-0.1525	-8.8294	0.00000000000000
0.062700	0.0173	-2.7694	-2.6493	-0.1201	-6.9525	0.00000000000179
0.064700	0.0173	-2.7380	-2.6493	-0.0887	-5.1346	0.00000014139150
0.066700	0.0173	-2.7076	-2.6493	-0.0582	-3.3720	0.00037316648427
0.068700	0.0173	-2.6780	-2.6493	-0.0287	-1.6614	0.04831265953555
0.070700	0.0173	-2.6493	-2.6493	0.0000	0.0000	0.5000000000000000
0.072700	0.0173	-2.6214	-2.6493	0.0279	1.6151	0.94685425371528
0.074700	0.0173	-2.5943	-2.6493	0.0550	3.1863	0.99927958209687
0.076700	0.0173	-2.5679	-2.6493	0.0815	4.7161	0.99999879784094
0.078700	0.0173	-2.5421	-2.6493	0.1072	6.2064	0.99999999972900
0.080700	0.0173	-2.5170	-2.6493	0.1323	7.6594	0.99999999999999
0.082700	0.0173	-2.4925	-2.6493	0.1568	9.0768	1.0000000000000000
Moderate (Sd <sub>2</sub> )	$\beta$	Ln(Sd <sub>2</sub> )	Ln( $\lambda$ )	Ln(Sd <sub>2</sub> )-Ln( $\lambda$ )	(Ln(Sd <sub>2</sub> )-Ln( $\lambda$ ))/ $\beta$	Probability
0.08900	0.0170	-2.4191	-2.2926	-0.1265	-7.4324	0.00000000000005
0.09100	0.0170	-2.3969	-2.2926	-0.1043	-6.1265	0.00000000044913
0.09300	0.0170	-2.3752	-2.2926	-0.0825	-4.8490	0.00000062029082
0.09500	0.0170	-2.3539	-2.2926	-0.0612	-3.5988	0.00015987166074
0.09700	0.0170	-2.3330	-2.2926	-0.0404	-2.3745	0.00878595227912
0.09900	0.0170	-2.3126	-2.2926	-0.0200	-1.1753	0.11994427473484
0.10100	0.0170	-2.2926	-2.2926	0.0000	0.0000	0.5000000000000000
0.10300	0.0170	-2.2730	-2.2926	0.0196	1.1522	0.87538455595129
0.10500	0.0170	-2.2538	-2.2926	0.0388	2.2823	0.98876357933326
0.10700	0.0170	-2.2349	-2.2926	0.0577	3.3910	0.99965183036853
0.10900	0.0170	-2.2164	-2.2926	0.0762	4.4792	0.99999625418490
0.11100	0.0170	-2.1982	-2.2926	0.0944	5.5476	0.99999998552218
0.11300	0.0170	-2.1804	-2.2926	0.1123	6.5970	0.99999999997902
0.11500	0.0170	-2.1628	-2.2926	0.1298	7.6279	0.99999999999999
0.11700	0.0170	-2.1456	-2.2926	0.1471	8.6411	1.0000000000000000
Extensive (Sd <sub>3</sub> )	$\beta$	Ln(Sd <sub>3</sub> )	Ln( $\lambda$ )	Ln(Sd <sub>3</sub> )-Ln( $\lambda$ )	(Ln(Sd <sub>3</sub> )-Ln( $\lambda$ ))/ $\beta$	Probability
0.10330	0.0206	-2.2701	-2.0956	-0.1745	-8.4839	0.00000000000000
0.10822	0.0206	-2.2236	-2.0956	-0.1280	-6.2223	0.00000000024492
0.11314	0.0206	-2.1791	-2.0956	-0.0836	-4.0614	0.00002439411620
0.11806	0.0206	-2.1366	-2.0956	-0.0410	-1.9924	0.02316426520826
0.12298	0.0206	-2.0957	-2.0956	-0.0002	-0.0079	0.49684683277586
0.12790	0.0206	-2.0565	-2.0956	0.0391	1.8987	0.97119963087214
0.13282	0.0206	-2.0188	-2.0956	0.0768	3.7334	0.99990553479332
0.13774	0.0206	-1.9824	-2.0956	0.1132	5.5013	0.99999998114864
0.14266	0.0206	-1.9473	-2.0956	0.1483	7.2071	0.99999999999971
0.14758	0.0206	-1.9134	-2.0956	0.1822	8.8552	1.0000000000000000
Collapsed (Sd <sub>4</sub> )	$\beta$	Ln(Sd <sub>4</sub> )	Ln( $\lambda$ )	Ln(Sd <sub>4</sub> )-Ln( $\lambda$ )	(Ln(Sd <sub>4</sub> )-Ln( $\lambda$ ))/ $\beta$	Probability
0.15112	0.0206	-1.8897	-1.6665	-0.2231	-10.8459	0.00000000000000
0.15868	0.0206	-1.8409	-1.6665	-0.1743	-8.4732	0.00000000000000
0.16624	0.0206	-1.7943	-1.6665	-0.1278	-6.2110	0.00000000026323
0.17380	0.0206	-1.7499	-1.6665	-0.0833	-4.0494	0.00002567345797
0.18136	0.0206	-1.7073	-1.6665	-0.0407	-1.9799	0.02385927961141